~~Need ERDA 1/27~~

COO 3459-8

RENSSELAER POLYTECHNIC INSTITUTE

Troy, New York

MASTER

CONTRACT No. AT(11-1)-3459

FATIGUE OF VANADIUM-HYDROGEN ALLOYS

August 15, 1975

Prepared by

K. S. Lee
and
N. S. Stoloff

DISCLAIMER

FATIGUE OF VANADIUM--HYDROGEN ALLOYS

K. S. Lee* and N. S. Stoloff

Rensselaer Polytechnic Institute
Troy, New York

Introduction

The influence of hydrogen on the tensile behavior of the group Va refractory metals: Ta, V, and Nb, has been widely studied. Hydrogen, both in solution and in the form of hydrides, strengthens these metals in certain critical temperature ranges, and low temperature ductility is known to be significantly reduced (1-3). However, there does not seem to have been similar concern directed to possible effects of dissolved or combined hydrogen on either fatigue life or cyclic deformation characteristics of refractory metals. The present work comprises an evaluation of the fatigue behavior of unalloyed polycrystalline vanadium, a vanadium-hydrogen solid solution alloy, and two alloys containing hydrogen in excess of the room temperature solubility limit. Tests have been conducted both in stress control and in strain control at room temperature. Fatigue lives of the various alloys have been correlated with microstructure, cyclic hardening data, and with fracture mechanisms deduced from metallographic observations and scanning electron fractography.

Materials and Specimen Preparation

Vanadium obtained from Wah Chang Corp. contained 115 ppm C, 90 ppm O, 85 ppm N, 5 ppm H. Three lots of material were employed; two were received in the annealed condition with a grain size of ∿ 60μ. The third lot was received in the cold-worked condition; it was annealed for 1 hr. at 1348°K in vacuum, then furnace cooled. All three lots of material were then annealed for 2 hrs. at 938°K in vacuum to give the final grain size of 90μ. Fatigue and tensile experiments have been performed on material with 1 cm gage length and 0.5 cm gage diameter.

The solubility limit of hydrogen in vanadium at room temperature has been reported to be about 500 ppm, (1,4,5) but there is some disagreement in the literature with this value. Based upon our own electron microscope and metallographic observations, we believe that 400 ppm may be just in excess of the solubility limit at room temperature. Two heat treatments were conducted in hydrogen to produce different volume fractions of hydrides, and a third to introduce hydrogen in solution. After the anneal to achieve constant grain size, a predetermined amount of hydrogen, produced by thermal decomposition of ZrH_2, was introduced into the vacuum system. Hydrogen was in contact with vanadium for two hours at 873°K; a slow cool to room temperature followed. The three levels of hydrogen introduced were approximately 132, 400 and 1000 ppm, see Table I. Oxygen contents unavoidably increased together with hydrogen contents. Microstructures of the 400 and 1000 ppm alloys, both of which contained hydrides, are shown in Fig. 1a) and b), respectively. There is a significant difference in size and volume fraction of hydride particles in the two cases. At 400 ppm, electron transmission measurements indicated hydride lengths all less than 10μ, while the 1000 ppm material exhibited hydride lengths of ∿ 60μ.

Tensile tests were carried out at 300°K at a strain rate of 0.5 min.$^{-1}$. Fully reversed tension-compression fatigue tests on vanadium and the three $V-H_2$ alloys were conducted on a closed-loop electrohydraulic machine. For stress-controlled tests, a sine wave at 20 cps was introduced. Strain-controlled tests were run with a triangular wave to maintain a constant strain rate; frequency was 0.2 to 1 cps, depending upon maximum strain.

Cyclic hardening was monitored during constant strain tests by an X-Y recorder. Thin foils for transmission electron microscopy were prepared by jet electropolishing in 20% H_2SO_4 in methanol.

Experimental Results

Tensile Tests

Tensile data for vanadium and the three alloys appear in Table II. Both 400 and 1000 ppm hydrogen produced substantial increases in yield and ultimate tensile strengths, but only the higher hydrogen level had a deleterious effect on ductility. The fracture mode, however, changed from dimpled rupture in unalloyed vanadium and V-132 ppm H_2, to cleavage in both hydrided alloys. The data of Table II were utilized to select cyclic stress and strain levels.

Table I. Chemical Analyses of $V-H_2$ Alloys

Alloy	H_2 (ppm)	O_2 (ppm)
V	5	90
V-132	132 ± 10	125 ± 10
V-400	400 ± 40	210 ± 20
V-1000	1000 ± 100	300 ± 30

Table II. Tensile Data for V-H_2 Alloys

Alloy	MN/m^2	0.2% σ_y ksi	MN/m^2	U.T.S. ksi	Total ε %	Uniform ε %
V	140	20	231	33	42	22
V-132	152.6	21.8	238	34	> 65	22
V-400	179.2	25.6	186.9	26.7	40	22
V-1000	190.4	27.2	294	42	24.4	18.6

Fatigue Tests

Fig. 2 is an σ-N plot for vanadium and the three alloys. Annealed vanadium demonstrates an endurance limit of about 126 MN/m^2 (18 ksi). Hydrogen in solution had a small effect on endurance limit but substantial increases in resistance to fatigue were noted at the 400 ppm and 1000 ppm levels. The effect is much larger than can be attributed to differences in tensile strength (Table II) as shown by plots of $\sigma_{max}/\sigma_{UTS}$ vs. N_f in Fig. 3. This ratio is about 0.55 for annealed vanadium, in reasonable agreement with typical levels of 0.6 for bcc metals, (6) but is on the order of 0.8 for both hydrided alloys. (When the data are normalized for differing 0.2% offset yield stresses, similar apparent strengthening is noted.)

Fig. 4 shows the results of strain-controlled cycling on vanadium and the alloys. A Coffin-Manson relation is approximately obeyed for the four materials;

$$\Delta\varepsilon_p/2 = \varepsilon_f' N_f^{\alpha} \tag{1}$$

little difference is noted between annealed vanadium and material containing 132 ppm H_2; however, both the exponent, α, and intercept, ε_f', (known as the fatigue ductility coefficient) of the hydride-containing alloys are decreased, see Table III. Calculations were done by subtracting elastic strain from the total strain values appearing in Fig. 4. Both 400 ppm and 1000 ppm H_2 produce nearly the same results, with lives distinctly inferior to that of annealed vanadium. This is undoubtedly a consequence of diminished tensile ductility, ε_f, in the presence of hydrogen, see Table II.

Cyclic hardening data for the four test materials at 300°K are summarized in Fig. 5. In all cases, hardening occurred in the first 10-100 cycles, followed by saturation. Cyclic stress-strain curves, obtained by plotting saturation stress vs. half of the reversed plastic strain (calculated assuming no effect of hydrogen on elastic modulus), are shown in Fig. 6. Monotonic stress-strain curves for the same materials also are shown. It is apparent that cyclic strain hardening is considerably more rapid than is monotonic hardening, and that hydrides at both levels produce a sharp increment in strength levels. However, the slopes, n', of the cyclic strain hardening curves, Fig. 5, decreased with increasing hydrogen content, see also Table III.

Table III. Effect of Hydrogen on Coffin-Manson Coefficients

Alloy	α	ε'_f	n'	$\frac{-1}{1 + 5n'}$
V	-0.49	0.29	0.33	-0.37
V-132	-0.35	0.13	0.297	-0.40
V-400	-0.39	0.066	0.159	-0.55
V-1000	-0.32	0.023	0.08	-0.71

To compare the results of stress-controlled and strain-controlled cycling tests, saturation stress values for specimens tested in strain control are plotted together with stress control data in Fig. 7. The two hydrided alloys reveal a discontinuity between stress and strain control data points, while the results for annealed vanadium are much more consistent. Data for the 132 ppm alloy (not shown) resemble those for annealed vanadium. In pure molybdenum there is a considerable discontinuity between σ-N curves obtained by the two methods, (7) although for fcc metals the σ-N curve is usually continuous (8). The presence of a discontinuity in molybdenum has been explained as due to the different frequencies used in the two types of tests (7). For molybdenum, the effect of an increase in frequency is to raise the apparent fatigue limit. The results of the present work indicate that the discontinuity is more pronounced for the hydrided alloys than for annealed vanadium or for a V-132 ppm H_2 alloy. Frequency effects in stress-control tests must be evaluated in order to determine whether they are indeed the cause of the observed discontinuities.

Metallographic Observations

Samples of vanadium and of V-132 ppm H_2 tested in stress control at low stresses revealed no secondary surface cracking; the primary crack mostly followed a transgranular path after initiating at slip bands. At high stresses, many secondary cracks along slip bands were seen, Fig. 8a) while the primary crack followed a mixed intergranular-transgranular path, see Fig. 8b). For material containing 400 ppm H_2, fracture was completely by transgranular cleavage; a few secondary cracks could be seen at grain boundary triple points, but no extensive network of cracks could be seen.

Hydrided samples of 1000 ppm hydrogen content exhibited small secondary cracks near the primary crack, Fig. 9. The relation between crack path and hydride morphology remains to be determined.

Fractographic Examination

Annealed vanadium, tested in either stress or strain control, revealed profuse striations as shown, for example, in Fig. 10a). Striations also were noted in 132 ppm H_2 material, but were interspersed with brittle regions, see Figs. 10b) and 10c). Samples with 1000 ppm H_2, on the other hand, revealed cleavage failure only both in stress and strain control, see Fig. 10d). 400 ppm H_2 material was anomolous, in that a few striations were noted in low stress, high cycle tests, while primarily cleavage was noted in high stress tests.

Discussion

The room temperature tensile and fatigue properties of vanadium are not markedly influenced by 132 ppm hydrogen. There is a small increase in the σ-N curve, which probably arises from the approximately 10% increase in yield stress produced by this level of hydrogen, and virtually no effect on low cycle fatigue life based on total strain. However, hydrogen in excess of the solubility limit produces two effects which appear at first glance to be mutually exclusive; there is a substantial increase in the tendency for transcrystalline cleavage in both tension and fatigue, yet fatigue lives in stress control are prolonged far in excess of what could be accounted for simply by an increase in montonic tensile properties. In strain control, however, hydrides produce a significant decrease in life, consistent with a reduced ductility in tension.

The increased high cycle life in the presence of hydrides may be connected with the decrease in n' (see Fig. 6) produced by hydrides. Feltner and Beardmore (9) have suggested that for increased stress resistance it is desirable to decrease n', while for increased plastic strain resistance it is best to increase n'. We note that the decreased n' produced by hydrides does lead to increased stress-cycling life, consistent with the Feltner-Beardmore analysis. However, when α and n' were compared as suggested by Morrow and Sinclair (10):

$$\alpha = -1/1 + 5n' \qquad (2)$$

no agreement was noted, see Table III. Consequently the role of n' is not yet fully understood.

The major effect of hydrides on crack path is to shift fracture from largely transgranular by ductile striation growth to wholly transgranular by a cleavage mechanism. Again the presence of 132 ppm H_2 in solution had little effect on fractographic features. It is noteworthy that this level of hydrogen is significantly higher than that needed to produce pronounced tensile embrittlement at low temperature (e.g. 100-200°K). However, the lack of correlation between high cycle fatigue life and fracture mode is consistent with the observation that large reductions in area or elongations can occur simultaneously with a cleavage fracture mechanism in refractory metals (3).

Summary

1. Hydrogen contents near and above the room temperature solubility limit increase the high cycle fatigue life, but decrease low cycle life of polycrystalline vanadium.

2. Changes in endurance limit with hydrides may be a consequence of decreased cyclic strain hardening coefficient, n'.

3. 132 ppm hydrogen in solution has only a slightly beneficial effect on stress controlled fatigue life and essentially no effect on low cycle fatigue life.

4. Unalloyed vanadium exhibits profuse striations, while hydrides produce cleavage cracks in fatigued samples.

Acknowledgements

The authors are grateful to the U. S. Energy Research and Development Administration (ERDA) for financial support under Contract No. AT(11-1)--3459.

References

1. C. W. Owen, D. H. Sherman and T. E. Scott, *Trans. Met. Soc. AIME*, 1967, Vol. 239, pp. 1666-1667.
2. D. G. Westlake, *Trans. Met. Soc. AIME*, 1969, Vol. 245, pp. 1969-1973.
3. H. K. Birnbaum, M. Grossbeck, and S. Gahr in *Hydrogen in Metals*, I. M. Bernstein and A. W. Thompson, Eds., American Society for Metals, 1974, pp. 303-323.
4. C. W. Owen and T. E. Scott, *Met. Trans. 3*, 1972, Vol. 3, pp. 1715-1726.
5. D. G. Westlake, *Trans. Met. Soc. AIME*, 1967, Vol. 239, pp. 1341-1344.
6. A. Ferro, P. Mazzette, and E. Montalenter, *Phil. Mag.*, 1965, Vol. 12, p. 867.
7. P. Beardmore and P. H. Thornton, *Met. Trans.*, 1970, Vol. 1, pp. 775-779.
8. P. P. Benhan, *J. Inst. Met.*, 1960/61, Vol. 89, p. 328.
9. C. E. Feltner and P. Beardmore, in ASTM STP 467, p. 77, American Society for Testing and Materials, Philadelphia, Pa., 1970.
10. J. Morrow and G. M. Sinclair, in ASTM STP 237, p. 83, American Society for Testing and Materials, Philadelphia, Pa., 1958.

Figure Captions

1. Microstructures of hydrided vanadium a) 400 ppm hydrogen, x1000 b) 1000 ppm hydrogen, x150.

2. σ-N data for stress-controlled cycling of vanadium and vanadium-hydrogen alloys.

3. σ-N data, stress-controlled cycling, normalized for ultimate tensile strength.

4. Low cycle fatigue data.

5. Cyclic hardening data from strain-controlled cycling.

6. Cyclic stress-strain curves derived from data of Fig. 5.

7. σ-N data from Fig. 2 compared with saturation stresses computed from strain-control tests.

8. Fatigue cracks in annealed vanadium tested in stress-control at relatively high stresses. a) ± 21 ksi, 9.7 x 10^4 cycles, x110 b) ± 25 ksi, 1.2 x 10^4 cycles, x150.

9. Secondary cracks adjacent to primary fatigue crack in V-1000 ppm H_2, cycled at ± 40 ksi, 9.1 x 10^4 cycles, x150.

10. Scanning micrograph of fatigue fracture surfaces: a) striations in annealed vanadium cycled at ± 19 ksi, $N_f = 5.6 \times 10^5$ cycles, x200 b) striations in 132 ppm alloy, x500 c) brittle fracture surface overlaid by striations, 132 ppm alloy, x100 d) cleavage facets in 1000 ppm alloy, cycled at ± 40 ksi, $N_f = 4.6 \times 10^4$ cycles, x100.

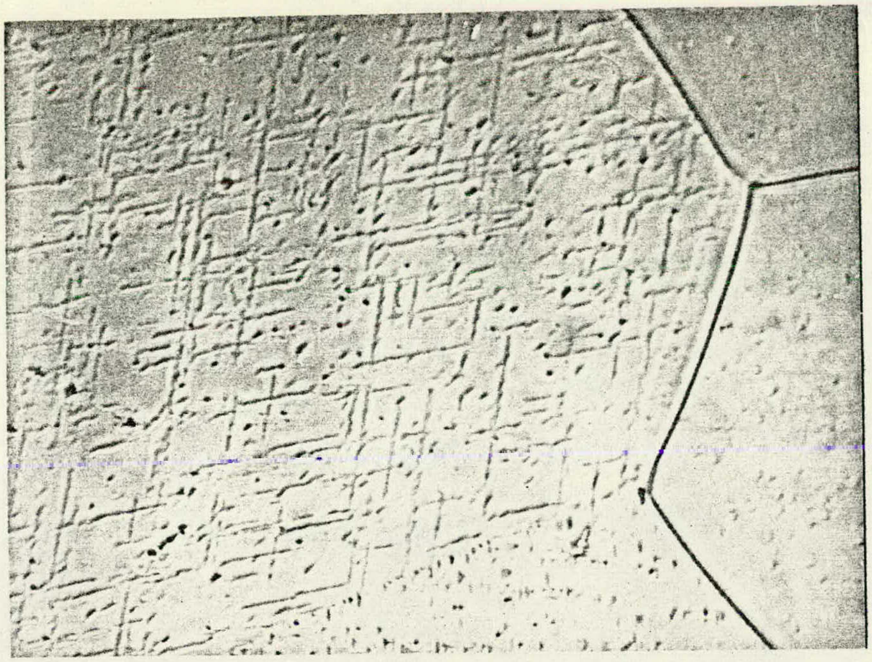

(a)

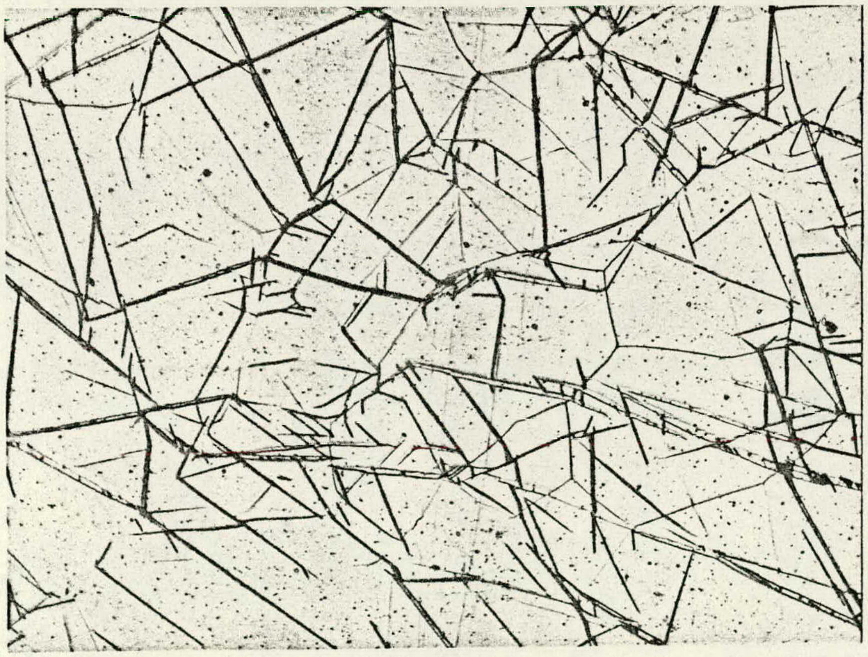

(b)

Fig. 1. Microstructures of hydrided vanadium a) 400 ppm hydrogen, x1000 b) 1000 ppm hydrogen, x150.

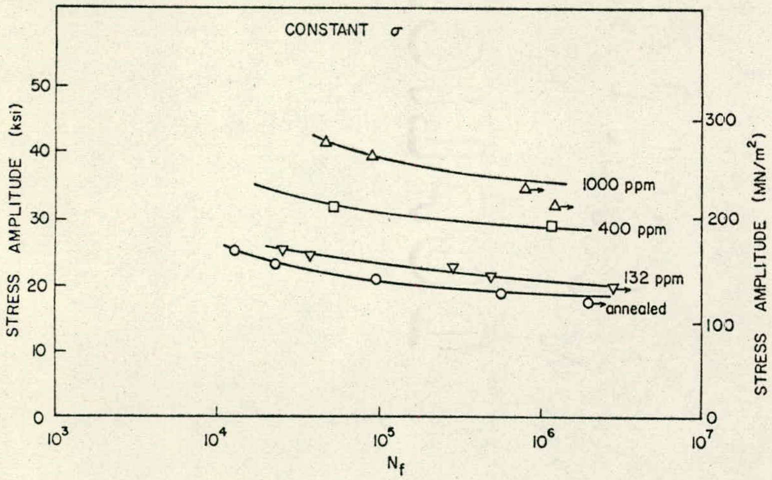

Fig. 2. σ-N data for stress-controlled cycling of vanadium and vanadium-hydrogen alloys.

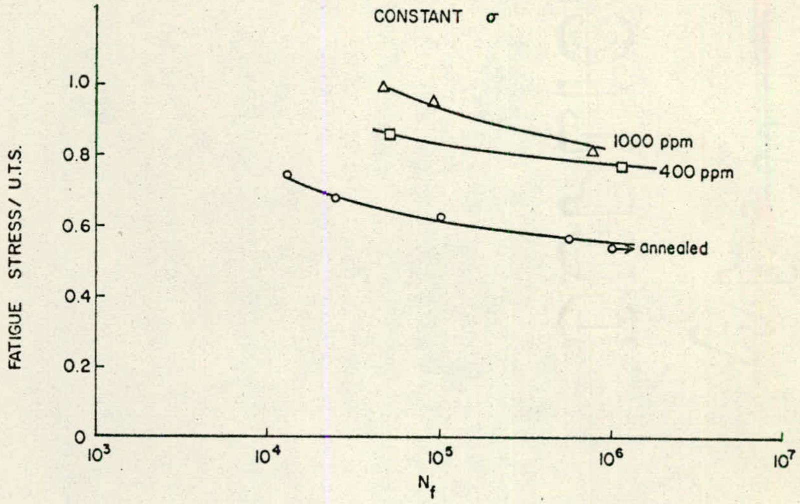

Fig. 3. σ-N data, stress-controlled cycling, normalized for ultimate tensile strength.

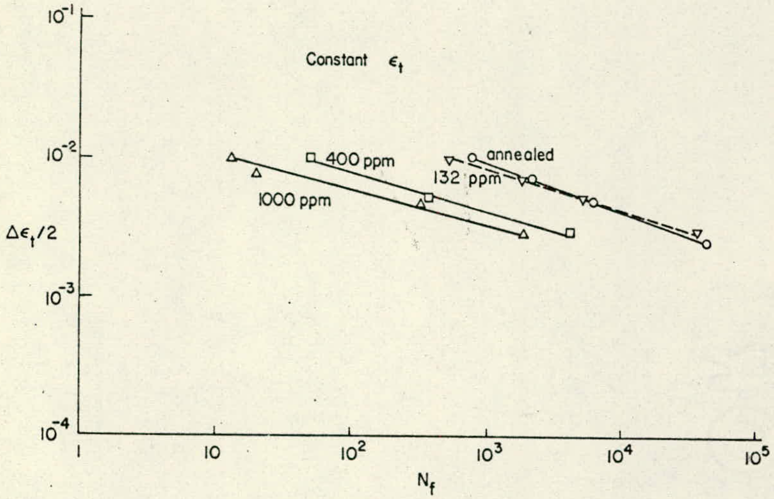

Fig. 4. Low cycle fatigue data.

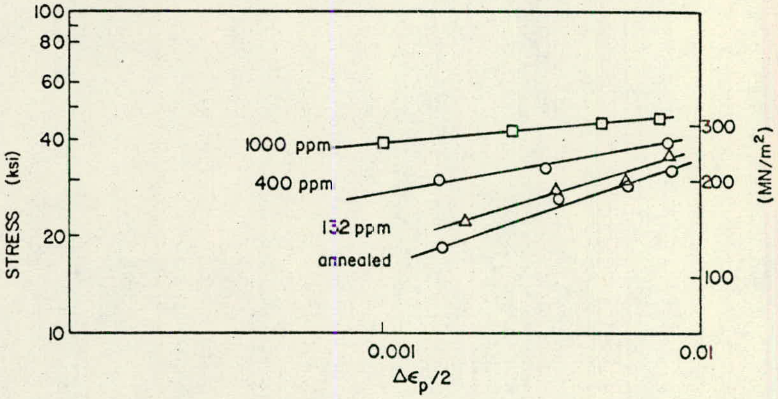

Fig. 5. Cyclic hardening data from strain-controlled cycling.

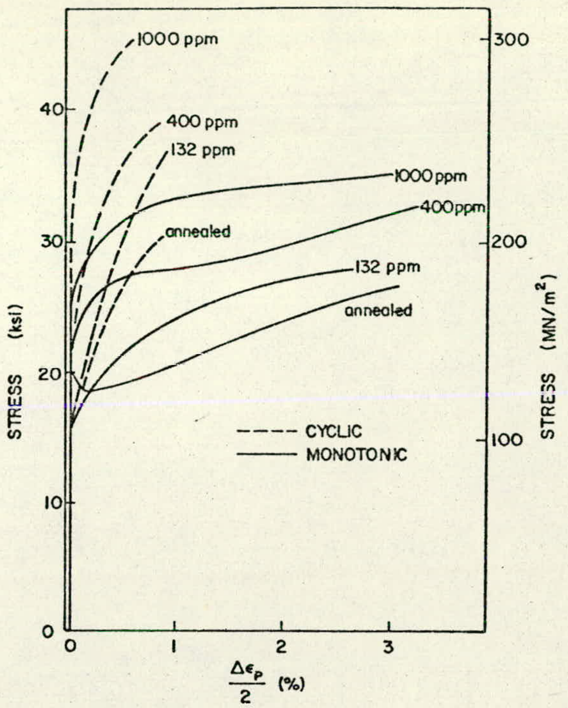

Fig. 6. Cyclic stress-strain curves derived from data of Fig. 5.

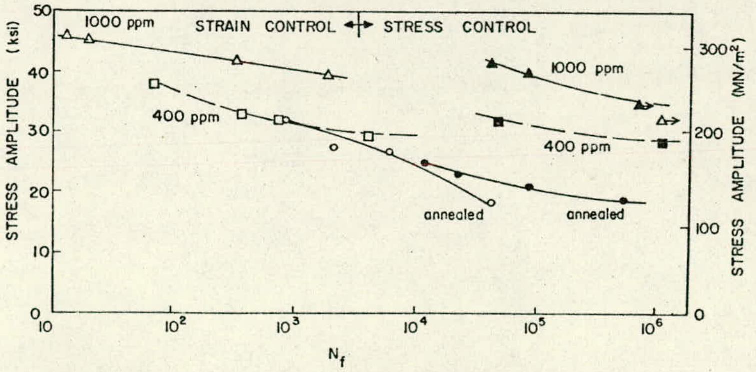

Fig. 7. σ-N data from Fig. 2 compared with saturation stresses computed from strain-control tests.

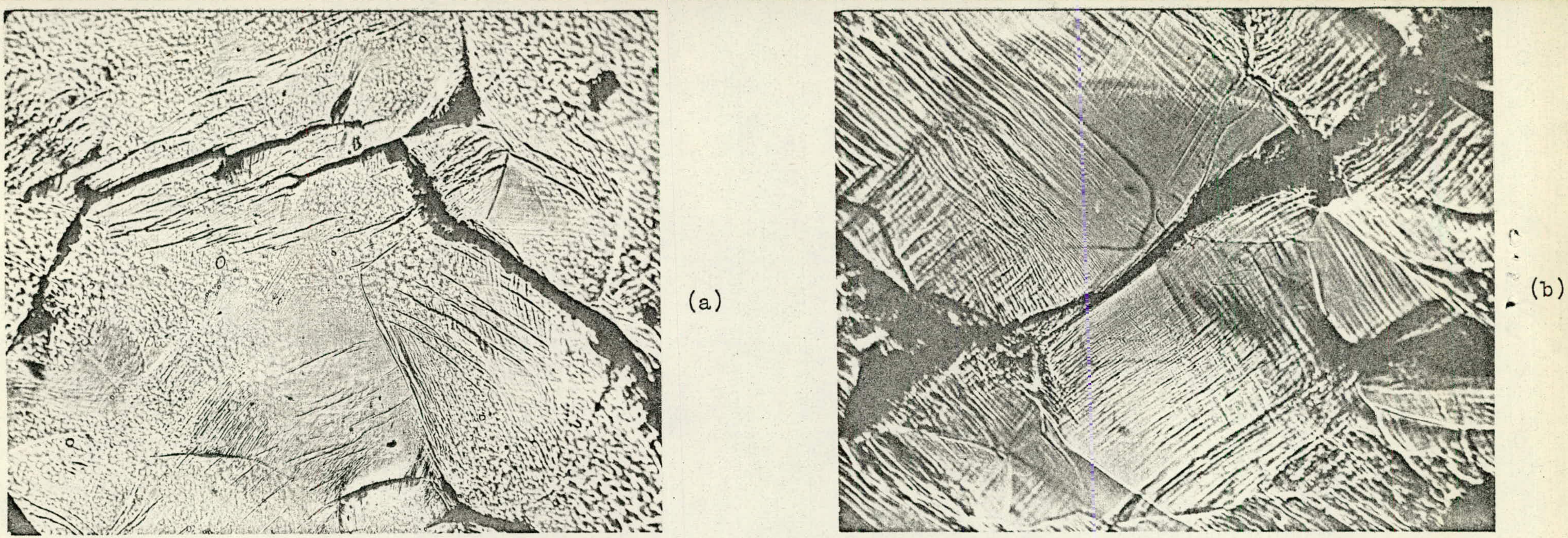

Fig. 8. Fatigue cracks in annealed vanadium tested in stress-control at relatively high stresses. a) ± 21 ksi, 9.7 x 10^4 cycles, x100 b) ± 25 ksi, 1.2 x 10^4 cycles, x 150.

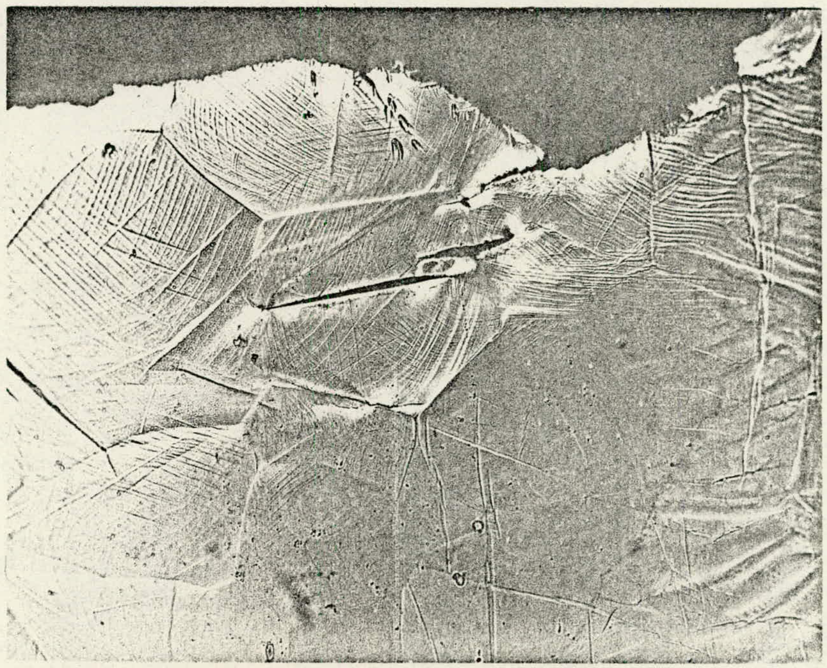

Fig. 9. Secondary cracks adjacent to primary fatigue crack in V-1000 ppm H_2, cycled at ± 40 ksi, 9.1 x 10^4 cycles, x150.

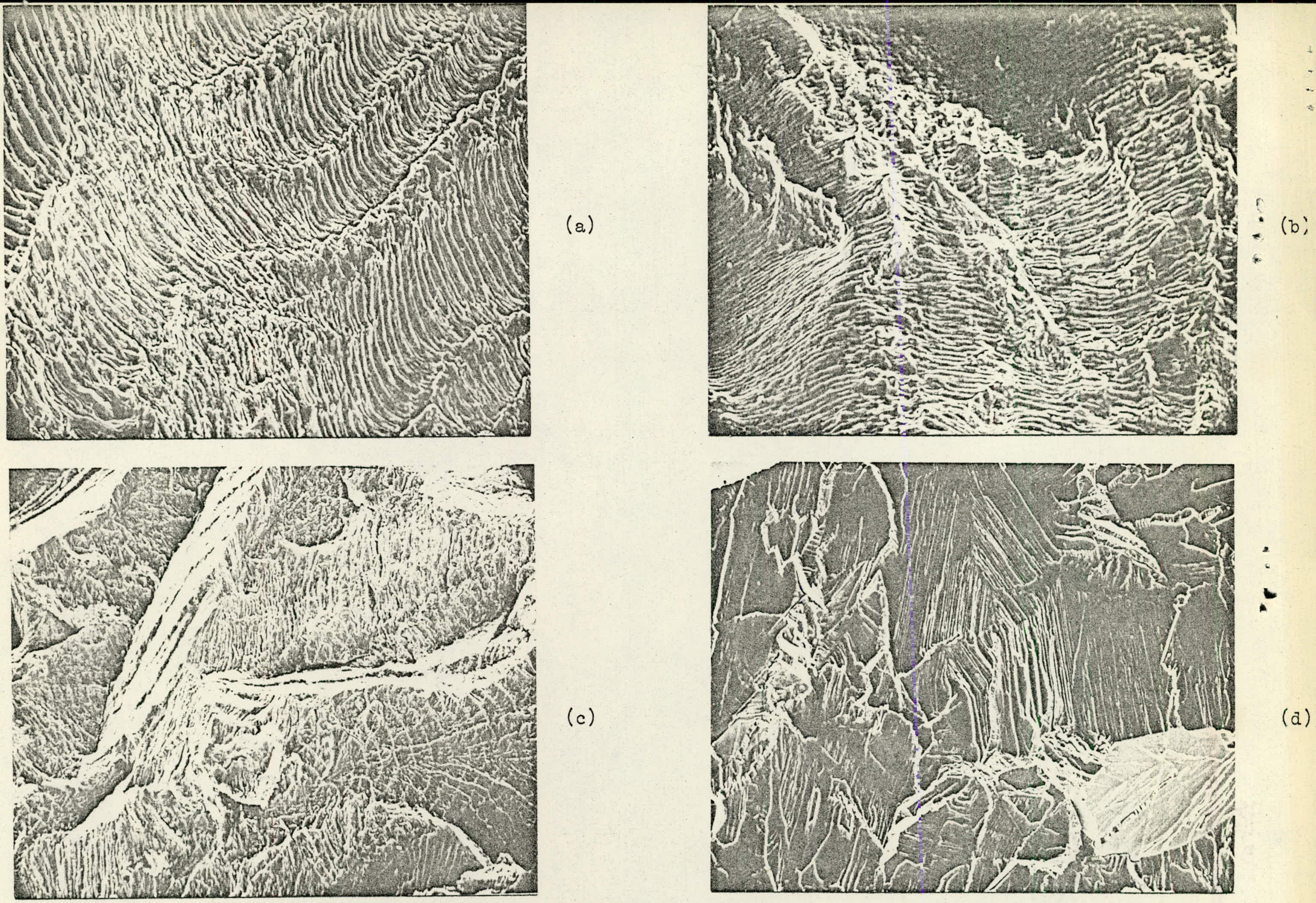

Fig. 10. Scanning micrograph of fatigue fracture surfaces: a) striations in annealed vanadium cycled at ± 19 ksi, $N_f = 5.6 \times 10^5$ cycles, x200 b) striations in 132 ppm alloy, x500 c) brittle fracture surface overlaid by striations, 132 ppm alloy, x100 d) cleavage facets in 1000 ppm alloy, cycled at ± 40 ksi, $N_f = 4.6 \times 10^4$ cycles, x100.